American Mineralogist, Volume 77, pages 795–809, 1992

Textural evidence of mafic-felsic magma interaction in dacite lavas, Clear Lake, California

JAMES A. STIMAC,* THOMAS H. PEARCE
Department of Geological Sciences, Queen's University, Kingston, Ontario K7L 3N6, Canada

ABSTRACT

At Clear Lake, California, the episode of volcanism from 0.65 to 0.30 Ma culminated in production of mixed dacite and rhyodacite lavas with bimodal phenocryst populations exhibiting extreme disequilibrium textures. These lavas formed by the interaction of subequal fractions of mafic recharge magma with the crystal-rich remnants of earlier-formed felsic magma bodies. The blending of basaltic andesite and rhyolite magmas dominated the early stages of mafic-felsic magma interaction. Partial quenching and segmentation of the resulting hybrid magma eventually led to the formation of quenched andesitic inclusions. During later stages of interaction, quenched inclusions suffered extensive disaggregation, contributing crystalline debris and residual silicic liquid to mixed dacites. The large range in mineral compositions and textures imply that given sufficient mafic input, preeruptive mixing is a remarkably efficient process, even in silicic magmas.

Phenocryst assemblages derived from the end-member magmas in dacite lavas preserve distinct compositions and styles of textural reequilibration. Felsic end-member phenocrysts responded to mixing mainly by dissolution and reaction recorded by (1) a rounded and embayed crystal form, (2) compositional reversals, (3) a partial reaction progressing inward from crystal margins, and (4) mantles or coronas that formed by diffusion-limited reactions in dissolution boundary layers. Sodic plagioclase derived from the felsic end-member shows a variety of features, including simple dissolution, abrupt shifts to more calcic composition, and fritted texture (representing a partial to complete reaction to more calcic compositions). Fritting occurs when sodic plagioclase experiences large changes in both liquid composition and temperature during residence in hybrid andesitic magma, whereas simple dissolution and calcic shifts occur when sodic crystals residing in felsic magma experience dramatic increases in temperature, followed by relatively small changes in liquid composition. Sanidine shows features analogous to plagioclase, including simple dissolution and shifts to more Ba-rich compositions. Some sanidine crystals are also mantled by plagioclase. Mafic end-member magmas (basaltic andesite) responded to mixing by combined liquid blending and undercooled crystallization, resulting in quenched andesitic inclusions and disseminated crystalline debris, with compositions intermediate between the end-member phenocryst populations. Plagioclase microphenocrysts formed during mixing are characterized by dendritic or skeletal growth forms and strong normal zoning. Calcic plagioclase phenocrysts present prior to mixing have abrupt sodic shifts and normal zoning at their margins, with rim compositions that match those of microphenocrysts in inclusions.

INTRODUCTION

Mafic-felsic magma interaction is now accepted as an important control on the chemical and textural diversity of igneous rocks, and some workers have suggested that magma mixing is the dominant process leading to the eruption of intermediate composition rocks in otherwise bimodal volcanic centers (Eichelberger, 1978; Grove and Donnelly-Nolan, 1986). Thus magma mixing may obscure the presence of compositional gaps in such systems, biasing our picture of them if left unrecognized. Determining the role of magma mixing in the origin of a given lava or suite provides insight into precursor magma compositions, their relative volumes, and the nature of their interaction in crustal magma chambers.

Our understanding of mafic-felsic magma interaction has been improved by numerous studies of variably mixed and mingled magmas (e.g., Wilcox, 1944; Anderson, 1976; Heiken and Eichelberger, 1980; Sakuyama, 1981; Bacon and Metz, 1984; Bacon, 1986; Frost and Mahood, 1987; Nixon and Pearce, 1987; Nixon, 1988a, 1988b; Clynne, 1989), as well as by theoretical and experimental assessments of the fluid dynamical, thermal, and chemical consequences of mafic-felsic magma interaction (Huppert et

* Present address: Los Alamos National Laboratory, EES-1, Geology/Geochemistry, Los Alamos, New Mexico 87545, U.S.A.

0003–004X/92/0708–0795$02.00

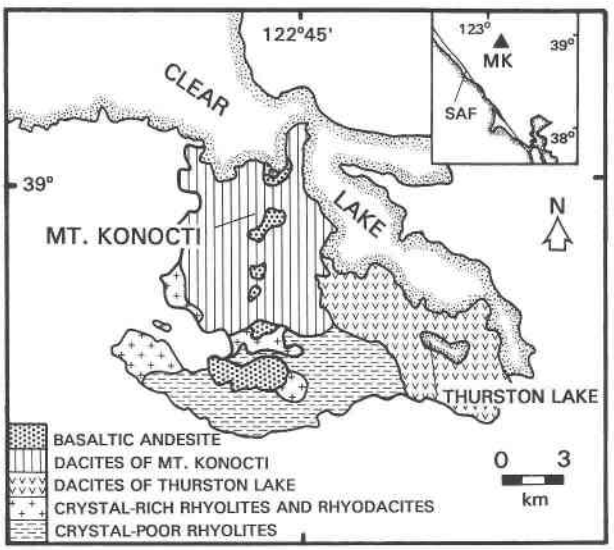

Fig. 1. Generalized geologic map of the Mount Konocti–Thurston Lake area, Clear Lake Volcanics, California (modified from Hearn et al., 1976). Only rocks from ~0.65 to 0.30 Ma are shown (structural detail omitted). Inset map shows the location of Mount Konocti (MK) relative to San Francisco Bay and the San Andreas fault (SAF).

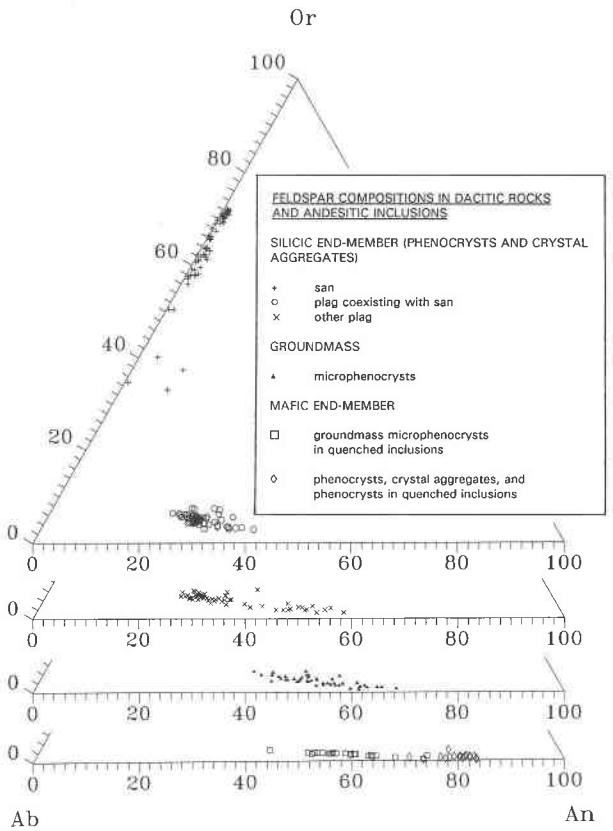

Fig. 2. Sanidine (san) and plagioclase (plag) compositions in dacitic lavas and andesitic inclusions from Clear Lake. Groupings are based on occurrence, composition, and texture, as described in text. See Table 2 for representative microprobe analyses of each textural type. End-member plagioclase phenocryst compositions average ~An_{30} and An_{80}, but some calcic zones and cores in otherwise sodic crystals range to An_{60}. Microphenocrysts in dacite lavas and quenched inclusions have overlapping ranges intermediate in composition between end-member phenocrysts.

al., 1982, 1984; Kouchi and Sunagawa, 1985; Koyaguchi, 1985; Sparks and Marshall, 1986; Turner and Campbell, 1986; Ussler and Glazner, 1989; Oldenburg et al., 1989). From these studies it is clear that the style of mafic-felsic magma interaction depends on the relative temperatures, compositions, and volumes of the magmas involved. When thermal and compositional contrasts between two magmas are large or the relative volume of mafic magma small compared to silicic magma, their interaction will be dominated by extensive crystallization of the mafic component, and little or no hybrid liquid will form (Bacon, 1986; Sparks and Marshall, 1986). In extreme cases, the small mafic input into rhyolitic systems is effectively quenched, with little evidence for liquid blending (Bacon and Metz, 1984; Stimac et al., 1990). Conversely, when the mass fraction of the mafic component is large (>30%) or where compositional differences are small (<10 wt% SiO_2), liquid blending will be more important (Kouchi and Sunagawa, 1985; Nixon and Pearce, 1987; Nixon, 1988a). Bacon (1986) used the term "mingled magmas" to differentiate occurrences dominated by undercooled crystallization of mafic magma in silicic magma from those where liquid blending is more important. Given sufficient mafic input into rhyolitic systems, mixing appears to occur in stages. The early stages are dominated by liquid blending and the formation of hybrid andesite, whereas in later stages, hybrid andesitic layers segment, forming quenched inclusions. Ultimately, disaggregation of inclusions may lead to fine-scale dissemination of inclusion debris in silicic magmas (Thompson and Dungan, 1985; Clynne, 1989; Stimac and Pearce, 1989), obscuring the distinction between liquid blending and mingling (as outlined above).

Study of the textures and compositions of minerals has proved to be the simplest and most effective means of establishing the role of magma mixing because minerals commonly preserve evidence of diverse and complex histories, even in magmas that are compositionally homogeneous. Furthermore, such study provides critical constraints on the nature of the mixing process itself. In this work we provide an inventory of textures and mineral zoning patterns in rhyodacite to dacite lavas from Clear Lake, California. These lavas represent preeruptive mixtures of subequal volumes of crystal-rich rhyolitic and basaltic andesite magmas. Emphasis is placed on the feldspars, because feldspar zoning and reaction textures provide a sensitive record of shifting magmatic conditions (Smith and Brown, 1988). The images used in this paper are of crystals from a number of dacitic units defined by Hearn et al. (1976, and unpublished data). Only a brief outline of rock and mineral compositions is given here. Sample locations, modal proportions, and ranges in rock

TABLE 1. Representative microprobe analyses of feldspars

	1	2	3	4	5	6	7
SiO_2	65.39	65.73	60.98	53.56	51.19	55.21	47.29
Al_2O_3	18.99	19.08	23.88	28.93	30.27	28.34	33.06
FeO*	0.05	—	0.09	0.11	0.27	0.44	0.42
CaO	0.18	0.10	6.06	12.13	14.08	11.54	17.42
Na_2O	4.09	3.21	7.49	4.72	3.56	4.98	1.89
K_2O	10.21	11.89	0.82	0.23	0.15	0.28	—
BaO	1.42	0.49	—	—	—	—	—
Total	100.33	100.50	99.32	99.68	99.52	100.79	100.08

Note: Analyses correspond to feldspar types in dacite lavas and andesitic quenched inclusions plotted in Figure 2. Numbers denote the following: 1 = san phenocryst rim ($Or_{62}An_1$) (crosses); 2 = san phenocryst core ($Or_{71}An_1$) (crosses); 3 = core of plag phenocryst ($An_{29}Or_5$) associated with san (circles); 4 = calcic zone in plag phenocryst core ($An_{58}Or_1$) (x's); 5 = plag microphenocryst ($An_{68}Or_1$) in dacite groundmass (filled triangles); 6 = plag microphenocryst ($An_{55}Or_2$) in quenched inclusion (squares); 7 = plag phenocryst ($An_{83}Ab_{17}$) in quenched inclusion (diamonds).
* All Fe as FeO.

and mineral compositions for individual dacitic units can be found in Stimac (1991).

Geologic setting

The Clear Lake Volcanics are located ~150 km north-northeast of San Francisco, California, within the broad San Andreas fault system. Volcanism at Clear Lake occurred in at least three episodes, with the greatest volume of silicic lava (rhyolite to dacite) erupted from 0.65 to 0.30 Ma (Donnelly-Nolan et al., 1981). Silicic units erupted from 0.65 to 0.30 Ma can be divided into several related sequences informally termed (1) crystal-poor rhyolites, (2) crystal-rich rhyolites, (3) dacites of Thurston Lake, and (4) dacites of Mount Konocti (Fig. 1). Rhyolites were erupted south and west of Mount Konocti from about 0.65 to 0.50 Ma (Donnelly-Nolan et al., 1981). The first rhyolites erupted were an extensive series (~6 km^3) of crystal-poor lavas, including the rhyolite of Thurston Creek (see Stimac et al., 1990). They were followed by the eruption of lesser amounts (<3 km^3) of crystal-rich rhyolite flows and tuffs (up to 33 vol% phenocrysts) along the southern and western margin of Mount Konocti. Volcanism culminated with the eruption of ~20 km^3 of rhyodacitic to dacitic lava in the Mount Konocti–Thurston Lake area from ~0.5 to 0.3 Ma (Donnelly-Nolan et al., 1981). The dacites of the Thurston Lake area (~3 km^3) form a series of coalescing flows and domes with K-Ar ages ranging from 0.48 to 0.44 Ma (Donnelly-Nolan et al., 1981). The dacites of Mount Konocti make up a composite volcano consisting mainly of lava flows and domes that rises 1000 m above the shore of Clear Lake. The dacites of Mount Konocti have an estimated volume of over 16 km^3 (Hearn et al., unpublished data) with K-Ar ages ranging from 0.43 to 0.26 Ma (Donnelly-Nolan et al., 1981). A lesser volume of mafic rocks is interbedded with the silicic sequences (Fig. 1).

Analytical methods

Microprobe analyses were conducted at Queen's University and Rensselaer Polytechnic Institute (RPI). EDS analyses of feldspars at Queen's were obtained on an ARL-SEMQ electron microprobe fitted with a Princeton Gamma Tech energy-dispersive spectrometer using a Tracor-Northern X-ray analysis system. Ten-element analyses were performed using an accelerating potential of 15 kV, a beam current of 100 nA, and count times from 100 to 200 s. A synthetic basaltic glass was used as a primary standard to calibrate the EDS spectrum. WDS feldspar and glass analyses done at RPI were obtained on a JEOL 733 Superprobe using an accelerating potential of 15 kV at a beam current of 15 nA and employing appropriate secondary standards. In both cases, X-ray intensities were corrected for matrix effects using the procedures of Bence and Albee (1968) and α correction factors of Albee and Ray (1970). Further details of the analysis procedure, precision, and accuracy can be found in Stimac (1991).

Interference imaging techniques used in this study have been described previously by Nixon and Pearce (1987) and Pearce et al. (1987) and are briefly noted below. Narrow-fringe laser interferometry and Nomarski differential interference contrast (DIC) studies were carried out in the Queen's University Laser Lab, as described by Pearce (1984a, 1984b). Nomarski DIC images were produced by viewing samples etched with fluorboric acid in reflected light (see Anderson, 1983; Pearce and Clark, 1989; for details of the technique).

Dacite lavas at Clear Lake

Dacitic rocks of the Mount Konocti–Thurston Lake area contain bimodal phenocryst assemblages exhibiting extreme disequilibrium textures consistent with an origin by magma mixing (Anderson, 1936; Brice, 1953; Hearn et al., 1981). Examination of the temporal trends, whole-rock compositions, and mineral assemblages and textures of other magmas erupted from 0.65 to 0.30 Ma (Fig. 1) indicate that the end-member assemblages in mixing events were derived from precursor rhyolitic and basaltic andesite to andesite magmas (Stimac, 1991). Despite partial reequilibration, precursor mineral assemblages can be identified based on their occurrence in crystal aggregates with distinctive compositions, grain sizes, and textures. The silicic assemblage consists primarily of coarse-grained sanidine (up to 2 cm), sodic plagioclase, quartz, Fe-rich pyroxene, biotite, and ilmenite. Mineral compositions and textures of this assemblage are nearly identical to those found in crystal-rich rhyolites erupted prior to the dacites (Stimac, 1991). The mafic assemblage consists primarily of finer-grained calcic plagioclase (typically <2 mm), Mg-

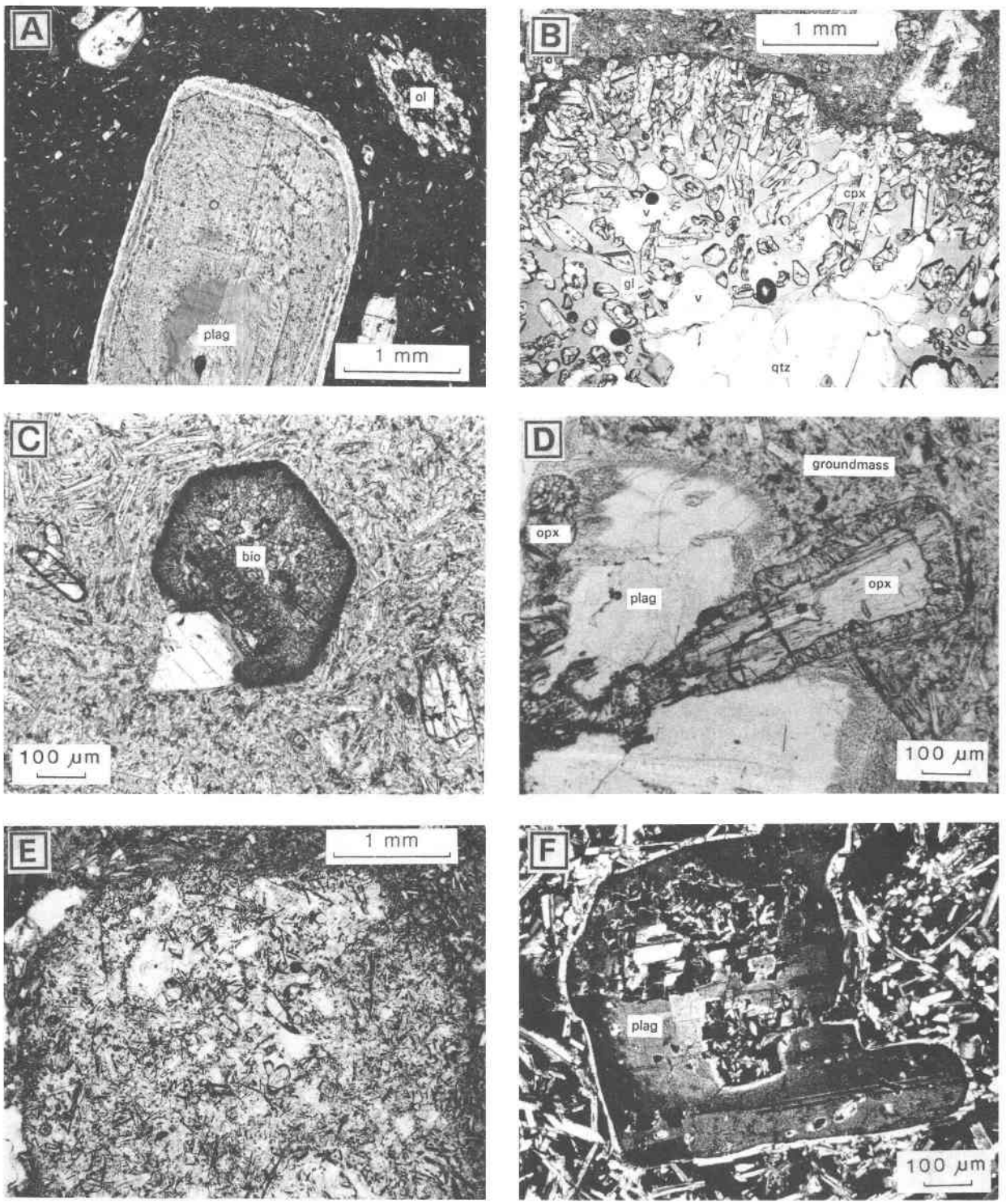

rich pyroxenes, and lesser olivine. The mineral compositions and textures of this assemblage are similar to those found in basaltic andesite lavas and andesitic quenched inclusions in rhyolitic rocks, but compositions of mafic minerals in individual units vary (Stimac et al., 1990; Stimac, 1991). Feldspar compositions for representative dacite lavas are summarized in Figure 2 and Table 1. Plagioclase phenocrysts clearly form two populations centered at An_{30} and An_{80}. Microphenocrysts in quenched inclusions and microphenocrysts in the groundmass of

←

Fig. 3. Textural features in dacite lavas from Clear Lake (plane polarized light and crossed nicols). Mineral composition based on microprobe analyses. Abbreviations for minerals in this and following figures are plagioclase, plag or P; sanidine, san or S; orthopyroxene, opx; clinopyroxene, cpx; biotite, bio; quartz, qtz; olivine, ol; ilmenite, ilm; glass, gl; and vesicle, v. See Stimac (1991) for more information on individual samples. **(A)** Large plag with a fritted exterior (~An_{47}) and sodic core (An_{28}; center) derived from the silicic end-member and Mg-rich olivine (Fo_{86}) rimmed by amphibole (upper right) (sample SCL-18C; dacite of Konocti Bay; DKB) derived from the mafic end-member. Reaction textures are interpreted as the result of magma mixing. **(B)** Augite corona on qtz (sample SCL-14A; dacite of Thurston Lake). The corona consists of bladed cpx with abundant interstitial glass. We interpret such coronas as forming by diffusion-controlled growth of cpx in a dissolution boundary layer on qtz (Sato, 1975) induced by magma mixing. **(C)** Pseudomorph after bio consisting of fine-grained oxides and silicates (sample SCL-37C; dacite of Vulture Rock; DV). Similar reaction products of bio in dacites were interpreted by Nixon (1988a) as resulting from dehydration above its stability limit attending magma mixing. **(D)** Fe-rich opx rimmed by more Mg-rich fine-fritted opx in a felsic crystal aggregate (sample SCL-9B; dacite of Soda Bay; DSB). Sodic plag in the aggregate shows fine-fritted texture at its margin. **(E)** Quenched andesitic inclusion in rhyodacite host (sample SCL-11B1; dacite of Benson Ridge; DBR). The inclusion contains Mg-rich pyroxene phenocrysts set in a groundmass of bladed plag, opx, opaques, and vesicular glass. **(F)** Fine-fritted plag in quenched inclusion thought to represent reaction products of a sodic phenocryst (sample SCL-10; DBR unit). Similar partially fritted crystals with sodic cores are common in andesitic inclusions and the rhyodacitic host. The crystal has a clear overgrowth ~An_{55} similar to plag microphenocrysts in the inclusions groundmass (Fig. 2).

the host dacites have broadly overlapping ranges intermediate in composition between the end-member phenocryst populations (Fig. 2).

Mineral assemblages and compositions are consistent with a history of episodic mafic recharge into the partly crystallized remnants of silicic magma bodies resulting in the production of hybrid dacite and rhyodacite lavas (Stimac and Pearce, 1989; Stimac, 1991). Whole-rock analyses of lavas and inclusions providing plausible end-member compositions are listed in Table 2. Mass balance tests that utilize these end-members yield good fits (R^2 from ~0.1 to 0.4), whereas crystal fractionation models invariably fail (Stimac, 1991). Successful mass balance models indicate that the fraction of mafic input ranged from ~30 to 60 wt%.

Observations

Textures of the silicic end-member phenocrysts

Phenocrysts derived from the silicic end-member in Clear Lake dacite lavas display a variety of disequilibrium textures (Fig. 3). Sodic plagioclase exhibits abrupt shifts to a more calcic composition and a fritted or sieve texture (Figs. 3A, 3D, 3F). Sanidine is invariably anhedral and embayed and is commonly mantled by plagioclase. Quartz is similarly rounded and embayed and commonly supports coronas of clinopyroxene (Fig. 3B). Biotite is anhedral to subhedral and rimmed or replaced by fine-grained intergrowths rich in titanomagnetite and pyroxene (Fig. 3C). Fe-rich orthopyroxene exhibits compositional reversals or is replaced by more Mg-rich orthopyroxene with a fine-fritted texture (Fig. 3D). Representative textures are described in more detail below.

Fine-scale plagioclase zoning. Zoning in plagioclase phenocrysts at Clear Lake can be divided into fine-scale oscillatory zoning and larger-scale compositional shifts superimposed on fine-scale patterns. Fine-scale zoning is thought to be controlled by the interplay of growth and diffusion rates in compositional and thermal boundary layers (unrelated to magma mixing) surrounding individual crystals (Sibley et al., 1976; Kuo and Kirkpatrick, 1982; Loomis, 1982; Pearce and Kolisnik, 1990). Fine-

Table 2. Representative whole-rock analyses of lavas and quenched inclusions

Sample	H76-17A	SCL-14D	SCL-11G	SCL-14	SCL-11	SCL-6
Unit	BK	DT/QI	DBR/QI	DT	DBR	RR
SiO_2	56.5	57.19	63.39	66.21	67.25	75.34
TiO_2	0.87	0.91	0.65	0.54	0.52	0.31
Al_2O_3	17.6	16.91	18.17	14.77	16.17	13.66
FeO*	5.57	5.19	3.88	3.26	3.14	1.46
MnO	0.09	0.08	0.06	0.07	0.06	0.03
MgO	5.8	5.56	2.61	2.57	1.80	0.30
CaO	8.7	7.09	5.34	3.75	4.16	1.20
Na_2O	3.1	2.88	3.84	3.35	3.73	3.60
K_2O	0.85	1.78	1.97	3.41	2.92	4.56
P_2O_5	0.23	0.15	0.09	0.10	0.15	0.02
LOI	0.78	2.25	0.40	1.70	0.80	0.40
Total	100.09	99.99	100.40	99.73	100.70	100.88

Note: LOI = loss on ignition. See Stimac (1991) for analytical methods. BK = basaltic andesite lava interbedded with dacite. DT/QI = quenched inclusion in dacite of Thurston Lake. DBR/QI = quenched inclusion in dacite of Benson Ridge (Mount Konocti). DT = dacite of Thurston Lake. DBR = dacite of Benson Ridge. RR = rhyolite of Red Hill Road.

* All Fe as FeO.

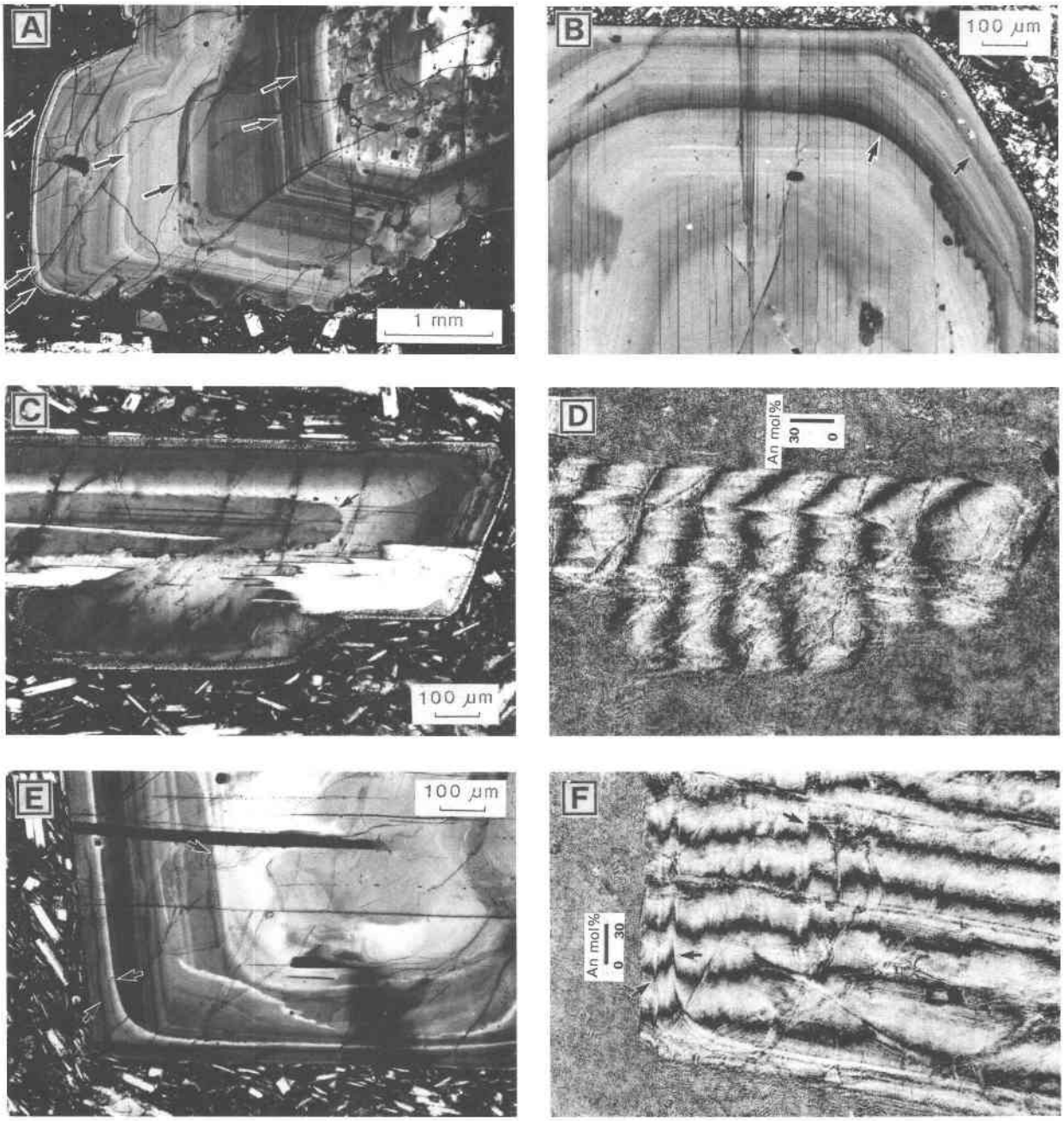

scale oscillations in plagioclase phenocrysts derived from the felsic end-member ($\sim An_{20-60}$; ave. An_{30}) at Clear Lake are typically 10–40 μm thick (see Figs. 4A, 4B). They appear to be broader, more diffuse, and of lower compositional amplitude than similar zones described from andesites (Nixon and Pearce, 1987; Pearce and Kolisnik, 1990). Large phenocrysts (Fig. 4A) commonly contain broad bands (up to 1 mm wide) consisting of numerous fine-scale zones, all with compositional variation of <5 mol% An.

Larger-scale plagioclase zoning. Larger-scale compositional discontinuities typically separate broad bands of fine-scale zones in silicic-derived crystals (Figs. 4A–4F). These discontinuities are commonly marked by evidence of erosion or truncation of underlying zones along a ragged interface (Figs. 4B, 4C). Such interfaces are typically followed by shifts to more calcic compositions (~5–15 mol% An; see Figs. 4D, 4F). Some crystals contain several such rounded interfaces, each followed by a marked shift to a more calcic composition (Fig. 4A). Steep normal zoning generally follows calcic shifts, with compositions becoming at least as sodic as in underlying zones (Figs. 4D, 4F).

Plagioclase reaction textures. In Clear Lake dacites,

←

Fig. 4. Plagioclase zoning patterns in felsic end-member crystals (crossed nicols and laser interferograms). Sodic plag phenocrysts in silicic rocks at Clear Lake are mainly from about 0.5 to 2.5 mm long, but some crystals range up to 2 cm. The compositional range of most crystals is small (<15 mol% An), but some crystals contain zones (usually cores) that are as calcic as An_{60} (Fig. 2, Table 1). The overall style of zoning is even to normal oscillatory, punctuated by calcic spikes (resorption surface, abrupt shift to more calcic composition, and strong normal zoning) that are thought to record magma mixing events (see discussion). (**A**) Plagioclase megacryst (~1 cm in length) recording a complex history of growth and resorption (sample SCL-9A; DSB unit). The crystal is oriented such that more calcic compositions show higher birefringence (lighter shades). The core is calcic (An_{49}) surrounded by a patchy zoned region (An_{29-50}). The rim is partially resorbed and has a thin calcic overgrowth ($>An_{50}$). The remainder of the crystal consists of broad sodic bands (An_{26-32}) with fine-scale oscillatory zoning, separated by resorption surfaces and compositional reversals of <5 to 15 mol% An (arrows). (**B**) Sodic plag with even to normal oscillatory zoning (compositional change across fine-scale oscillations are <5 mol% An) cut by two ragged interfaces (arrows) that truncate underlying zones (sample SCL-9E; DSB unit). The crystal is oriented such that more calcic compositions show lower birefringence (darker shades). Compositional reversals occur outside of each interface, with the maximum compositional shift being ~10 mol% An (arrows). (**C**) Sodic plag with a pronounced calcic spike at arrow (sample SCL-11B2; DBR unit). The crystal is oriented such that calcic compositions show higher birefringence (lighter shades). The crystal is fritted at its margin, with a thin overgrowth of calcic plag. (**D**) The laser interferogram of the grain in **C** records a compositional reversal of 5–10 mol% An, followed by steep normal zoning to the fine-fritted margin. (Laser interferograms consist of a series of parallel fringes that are shifted across zones of different refractive index—a shift of one full fringe measures a compositional change of ~32 mol%.) (**E**), (**F**) Sodic plag with a more complicated zoning history that includes abrupt shifts (>5 mol%) to both more calcic (higher birefringence) and more sodic compositions (sample DCJ-86-22B; DKB unit). The pronounced calcic spike near the edge of the crystal (outer arrow) is ~15 mol% An.

some sodic plagioclase crystals are partially fritted or sieve textured (Figs. 3, 5). Fritted and unfritted grains may occur side by side in dacite lavas, but virtually all crystals in andesitic inclusions with sodic cores have fritted exteriors. Some fritted crystals in inclusions (and less commonly in dacites) consist entirely of sieve-textured plagioclase (Fig. 3F). Fritted zones consist of an intergrowth of plagioclase and glass with a highly variable morphology (Figs. 5B–5D). When fritting is sufficiently coarse to obtain reliable microprobe analyses, compositions generally range from An_{50} to An_{80}. Most fritted crystals have clear, normally zoned overgrowths (Fig. 5C) ranging from ~An_{45} to An_{65}. The fritted texture typically truncates underlying zones, and in some crystals the size of the glass inclusions decreases inward (Figs. 5A, 5B).

Sanidine zoning. Sanidine in silicic lavas at Clear Lake has a limited range in composition, with the style of sanidine zoning being similar to that of sodic plagioclase. When the celsian component is excluded, sanidine cores range from Or_{68} to Or_{72}. However, rims of strongly reacted crystals may be as sodic as Or_{38} (Fig. 2). These more sodic compositions are present around crystal margins, embayments, and cracks and probably result from alkali exchange during and following mixing events (Fig. 6B). When these areas are excluded, zoning in sanidine is largely restricted to Ba and to a lesser extent, Ca. BaO concentrations range from about 0.4 to 1.8 wt% in a typical megacryst, with the largest increases occurring in areas outside of rounded interfaces that truncate underlying zones (Fig. 6A). Individual zones are typically broad (from 20 to 500 μm thick), diffuse, and separated by rounded interfaces.

Sanidine reaction and plagioclase mantle textures. Sanidine in Clear Lake dacitic and rhyodacitic rocks is invariably either rounded and embayed, mantled by plagioclase, or both (Figs. 6B, 6C). Plagioclase mantles have a variety of forms and sizes, summarized in Figure 6. Coarse plagioclase mantles (0.5–1.0 mm thick) typically consist of cellular-textured grains, whereas fine mantles are commonly bladed (compare Figs. 6C, 6D). Plagioclase mantles are generally optically continuous and have a preferred optical orientation to sanidine. Locally, it can be seen that the plagioclase of the mantle is separated from the underlying sanidine by a thin zone of clear glass (<0.25 mm). Fine-bladed mantles are typically continuous on their outer projection but taper inward, terminating in glass-filled channels in sanidine (Fig. 6D). Coarse-cellular plagioclase mantles have zoning that includes repeated compositional reversals. Compositions of mantles range from about An_{22} to An_{40} (Fig. 2).

Sanidine is rare in quenched inclusions, but when present, it is typically embayed and contains numerous ovoidal cavities. Plagioclase mantles on sanidine in inclusions commonly have a fine-fritted texture on their outer margins.

Augite coronas on quartz. Quartz grains with augite coronas are common in dacites at Clear Lake. Coronas consist of radially oriented bladed mats of clinopyroxene separated from quartz and the surrounding dacite by interstitial vesicular glass (Fig. 3B). Rimmed and unrimmed quartz phenocrysts commonly exist side by side in dacite lavas, whereas quartz crystals in quenched inclusions rarely lack coronas. Fragments of multigrained aggregates of acicular clinopyroxene with interstitial glass are also abundant in dacites, whether or not clinopyroxene occurs as phenocrysts. Corona fragments are most abundant when other felsic end-member minerals (sanidine, plagioclase, biotite) are also strongly resorbed. Augite in the coronas has a large compositional range, with the most Mg-rich compositions being similar to augite phenocrysts derived from the mafic end-member. Interstitial glass in coronas is commonly silicic (Stimac, 1991).

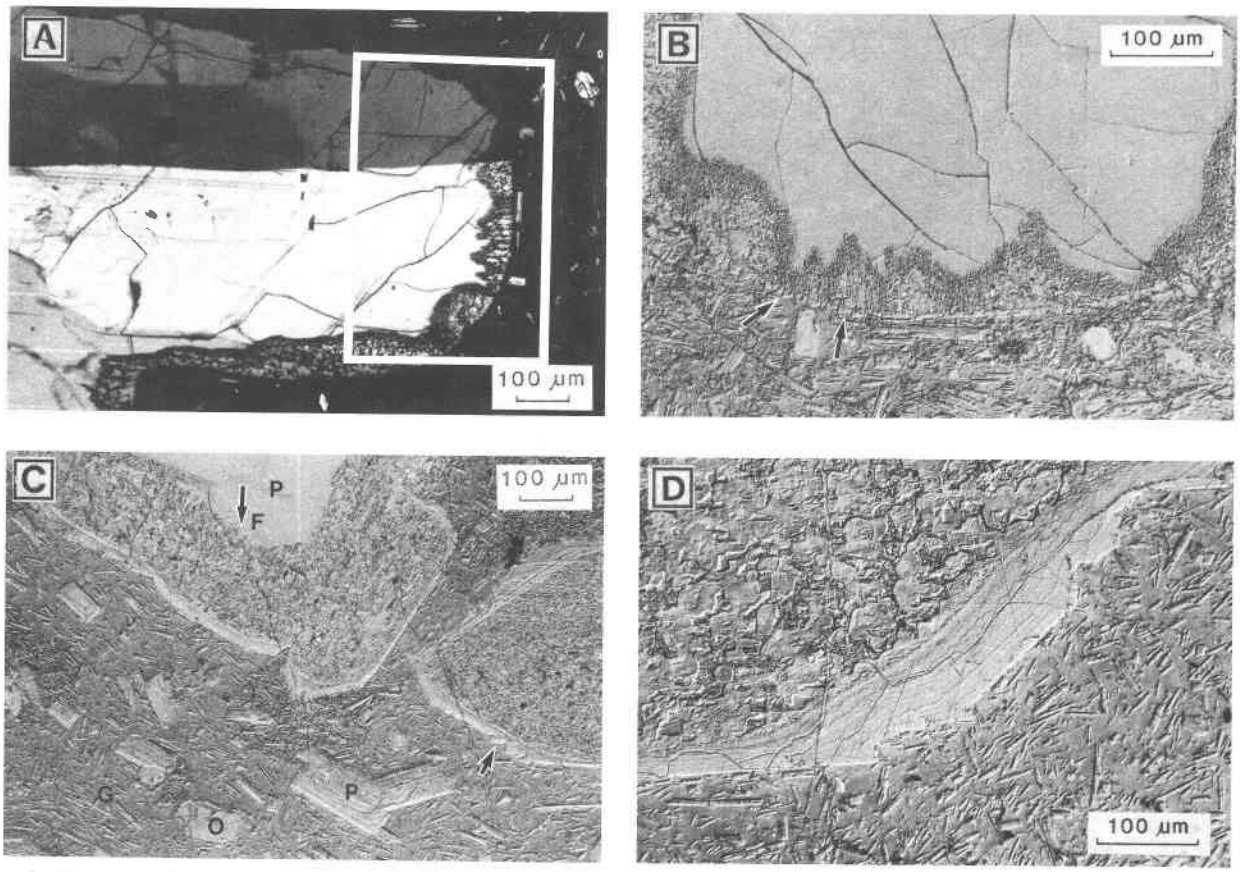

Fig. 5. Plagioclase reaction textures in the felsic end-member (Nomarski DIC images). Nomarski interference imaging yields an undistorted view of plagioclase-glass intergrowths in two dimensions and provides a qualitative estimate of changes in plagioclase composition too small to analyze with the microprobe (Pearce and Clark, 1989). (**A**), (**B**) Sodic plag with a fine-fritted rim that appears to coarsen outward (sample SCL-17C; DPF, dacite of Plum Flat). Reaction has proceeded inward from the crystal margin, producing an open framework of more calcic plag and interstitial glass. The coarser-grained intergrowth of plag and glass outside of the fine-fritting may have formed by rapid growth (arrows in **B**). (**C**) Plagioclase phenocryst consisting of (1) a sodic core, (2) a region of fine-fritting that truncates earlier formed zones (arrow at F), and (3) an overgrowth of more calcic composition (sample SCL-55E; DHP, dacite of Henderson Point). A neighboring plag consists of a fritted core and calcic overgrowth. In both crystals the overgrowths have skeletal projections that suggest rapid growth. Note that the groundmass is texturally heterogeneous. (**D**) Coarse-fritted core with clear calcic overgrowth (sample SCL-14E; DT unit).

Textures of the mafic end-member

Mafic end-member textures include those of phenocrysts in mafic crystal aggregates and quenched inclusions, as well as those of microphenocrysts in quenched inclusions. In laser interference profiles, calcic plagioclase phenocrysts are seen to have abrupt shifts to more evolved compositions at their margins such that rim compositions match those of plagioclase microphenocrysts in inclusions. Mg-rich olivine (Fo_{80-88}) is invariably rounded and rimmed by orthopyroxene or amphibole of the same composition as in the groundmass of inclusions (Fig. 3A). Plagioclase, pyroxene, and amphibole microphenocrysts forming the groundmass of quenched inclusions exhibit strong normal zoning and are characterized by dendritic or skeletal growth forms (Figs. 3E, 3F). Clino- and orthopyroxene microphenocrysts commonly occur as parallel intergrowths (Stimac, 1991). Zoning patterns of calcic plagioclase phenocrysts are described in more detail below.

Plagioclase zoning. Calcic plagioclase phenocrysts derived from the mafic end-member (Fig. 7) in mixed dacites have zoning patterns indicative of two very different stages of growth. Crystal cores have a restricted compositional range ($\sim An_{70-84}$; Fig. 2) and fine-scale even-oscillatory zoning (Figs. 7B, 7D). Cores are jacketed by more sodic rims ($\sim An_{50-65}$; not plotted in Fig. 2) that are normally zoned and have skeletal or dendritic morphologies. The contact between core and rim is usually sharp and marked by a shift to more sodic compositions (10–25 mol% An). In addition, the normally zoned region commonly contains one episode of reverse zoning shortly after the initial normal shift. This pattern of discontinuous zoning is almost identical to that observed in large crystals in quenched inclusions in earlier erupted rhyolites at Clear Lake (Stimac et al., 1990).

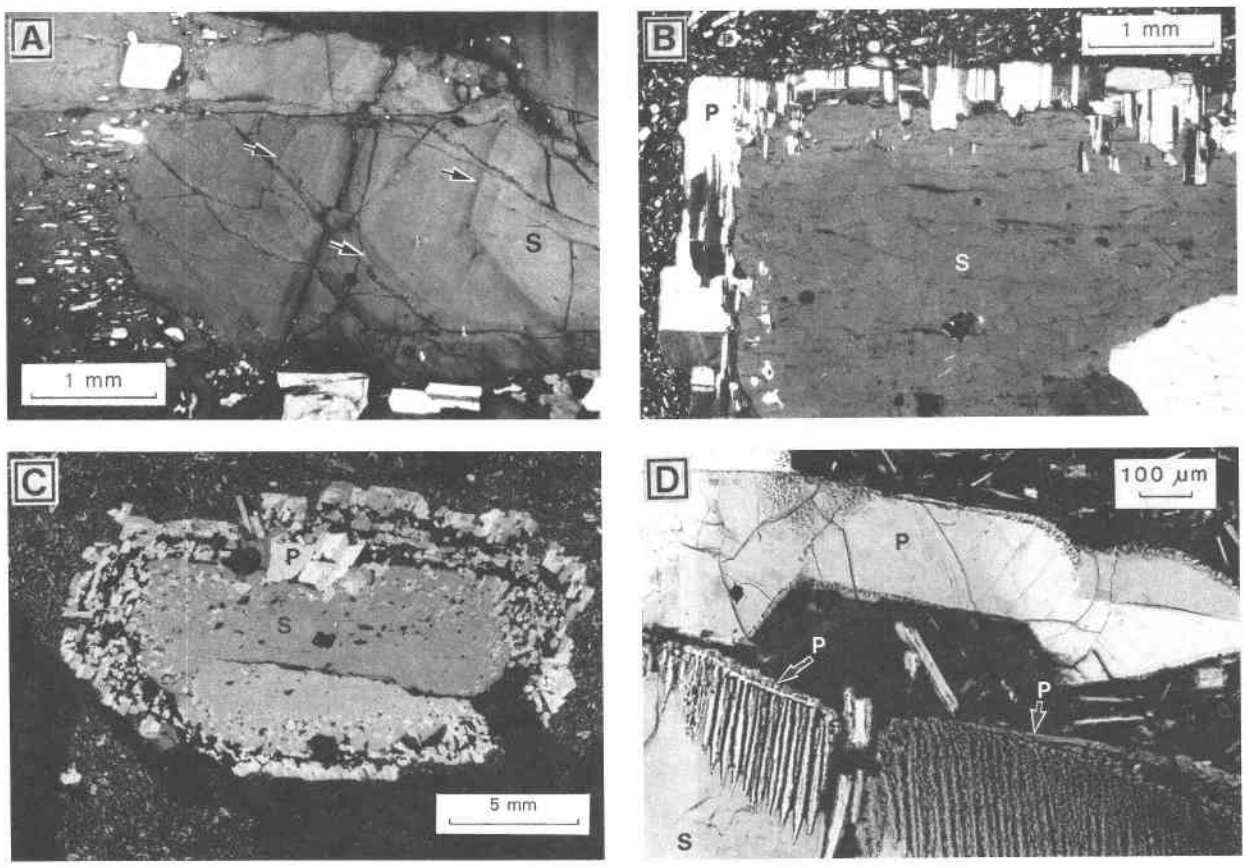

Fig. 6. Sanidine zoning and reaction textures (crossed nicols). Individual crystals range up to 2 cm in length, but most are several millimeters to 1 cm long. When the celsian component is excluded, sanidine cores range from Or_{68} to Or_{72}, whereas rims may be as sodic as Or_{38} (Fig. 2, Table 1). (**A**) Zoning in san megacryst with plag inclusions and fine-bladed plag mantles at its margin (not shown) (sample SCL-42F; DWP, dacite of Wright Peak). Optical zoning results mainly from changes in Ba concentration. Lower birefringence (darker shades of gray) are regions on higher Ba concentration. Each increase in Ba (arrows) is deposited on a rounded interface that truncates earlier formed zones. (**B**) Coarse plag mantles on san (sample DCJ-86-22B; DKB unit). Note the slight increase in birefringence at the sanidine margin, which corresponds to a region of higher Na. (**C**) Coarse-cellular plag mantle on san with abundant interstitial glass (sample SCL-11A; DBR unit). Plagioclase inclusions in san are in optical continuity with the rim. (**D**) Coarse-grained (upper) and fine-bladed (lower) plag mantles on san (sample SCL-9A; DSB unit). Note the continuous layer of plag normal to blades near the outer margin of the finer-grained mantle (arrows).

Discussion

Silicic end-member

Large-scale plagioclase zoning. Rounded interfaces, like those found in sodic plagioclases in silicic rocks at Clear Lake, are a common feature of plagioclase and have been interpreted as dissolution surfaces that formed during episodes of plagioclase resorption (Homma, 1932, 1936; Phemister, 1934; Nixon and Pearce, 1987; St. Seymour et al., 1990; Kolisnik, 1990; Pearce and Kolisnik, 1990). This interpretation is also in accord with the experimental evidence of Tsuchiyama (1985), who found that when a melt is undersaturated in plagioclase (above the liquidus for that particular melt composition), plagioclase undergoes simple dissolution, leading to rounded crystals. The combination of a rounded or ragged discontinuity (resorption surface) truncating underlying zones followed by a shift to a more calcic composition and subsequent normal zoning has been observed in numerous studies of plagioclase zoning in andesitic and dacitic rocks (Nixon and Pearce, 1987; Pearce et al., 1987; St. Seymour et al., 1990; Kolisnik, 1990; Blundy and Shimizu, 1991). This zoning pattern has been referred to as a "calcic spike" (e.g., Fig. 4E). In rocks with other petrographic and chemical evidence for mafic-felsic magma interaction, this general pattern has been attributed to shifts in temperature and melt composition attending magma mixing (Nixon and Pearce, 1987; Kolisnik, 1990). If calcic spikes record mixing episodes, then multiple reversals imply repeated mixing events.

Plagioclase reaction textures. Numerous petrographic studies have suggested that a fritted or sieve texture in plagioclase results from the reaction of sodic crystals to a more calcic composition (Kuno, 1950; Anderson, 1976; Nixon and Pearce, 1987). Furthermore, several experimental studies have confirmed that a fritted texture forms when sodic plagioclase is immersed in a melt that is in

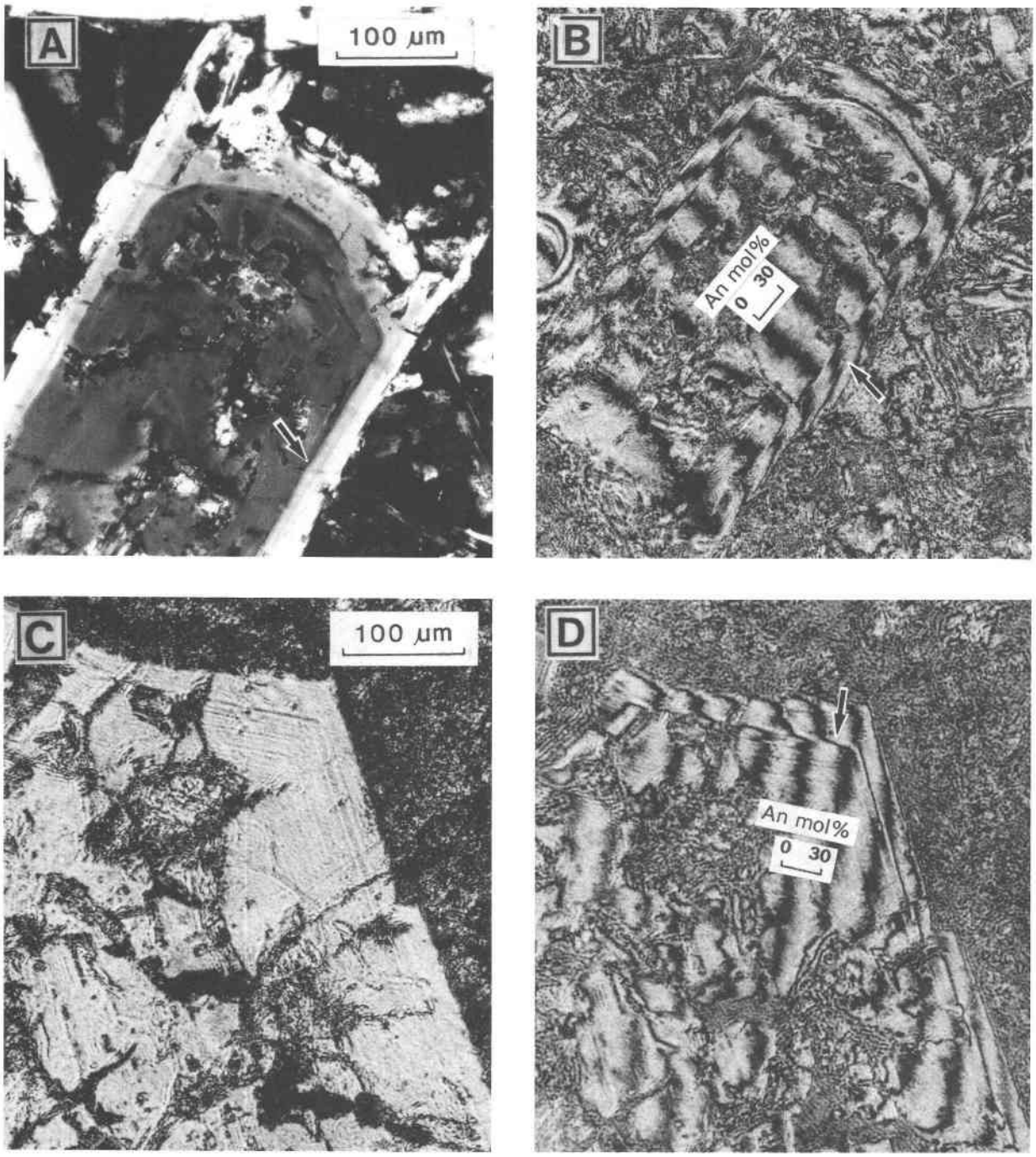

Fig. 7. Plagioclase zoning patterns of the mafic end-member under crossed nicols and as laser interferograms. (**A**), (**B**) Phenocryst in a quenched inclusion (sample SCL-9C; DSB unit). Zoning in the crystal core is even oscillatory (An_{80-84}). There is a sharp interface between core and rim, marked by a sodic shift of ~20 mol% An (arrow in **A**). The rim shows strong normal zoning with a small compositional reversal (arrow in **B**). (**C**), (**D**) Calcic plag in dacitic host with an even oscillatory–zoned core, sharp interface, and sodic shift followed by a small compositional reversal (arrow), within a normally zoned rim (plane polarized light and laser interferogram) (sample SCL-9A; DSB unit).

equilibrium with more calcic plagioclase (Lofgren and Norris, 1981; Tsuchiyama, 1985; Glazner et al., 1988, 1990). Alternatively, some authors have suggested that a fritted texture may form in plagioclase by rapid growth, during episodes of undercooled crystallization (Hibbard, 1981; Anderson, 1984). Kuo and Kirkpatrick (1982) described fritted crystals compatible with both origins.

Several criteria may be used to differentiate between

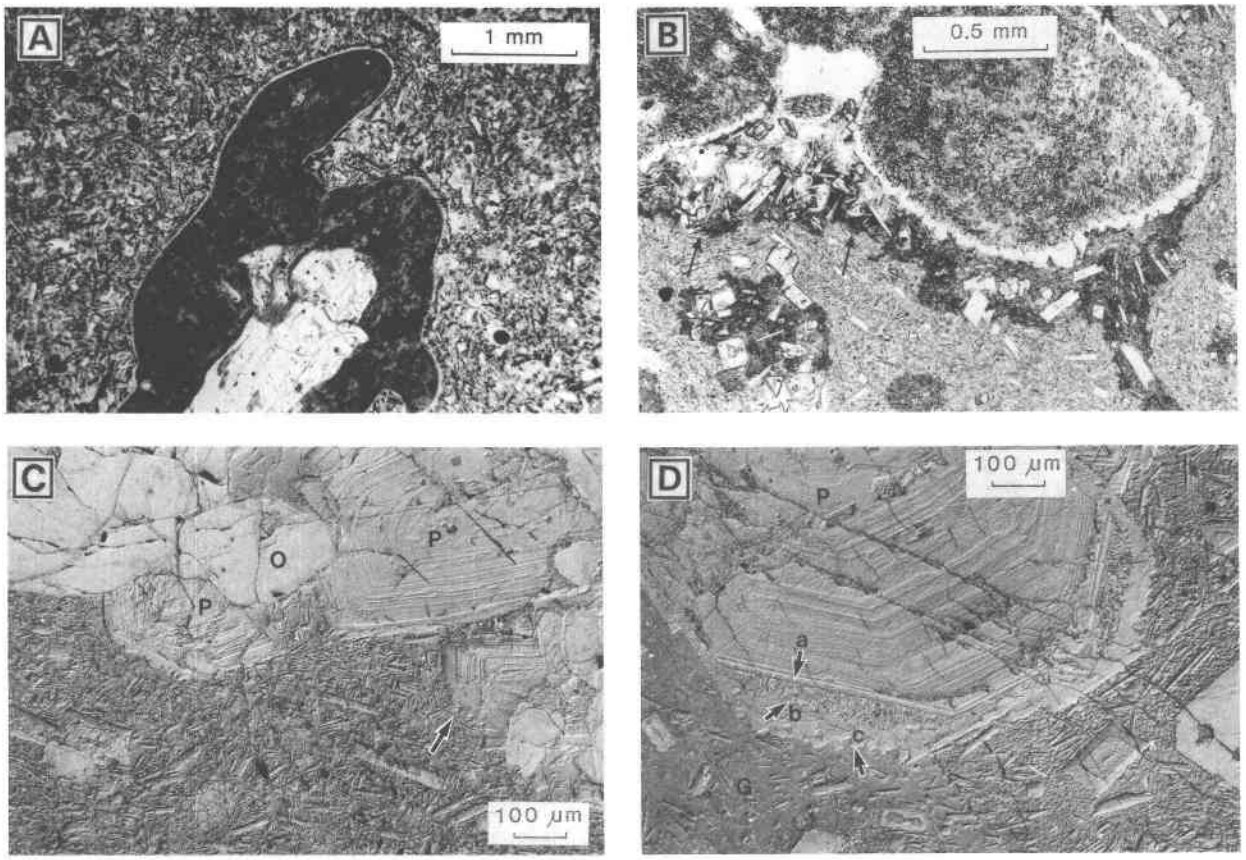

Fig. 8. Comparison of resorption and rapid growth textures in plagioclase from Clear Lake dacite lavas and andesitic inclusions. (**A**) Sodic plag crystal in a hybrid andesitic inclusion (sample SCL-11G; DBR unit). The crystal consists of a sodic core (An_{35}), fine-fritted region (more calcic), and a clear rim with skeletal outgrowths (An_{54}). (**B**) A plag crystal with a fine-fritted interior and clear calcic overgrowth similar to crystal in **A** but with remnants of quenched inclusion groundmass (arrows) preserved in an embayment (sample SCL-55E; DHP unit). (**C**) Portion of a mafic crystal aggregate in a dacite host consisting of plag and pyroxene (sample SCL-9B; DSB unit). Plag exhibits fine-scale even oscillatory–zoned cores (An_{78-84}) and an abrupt shift to more sodic rims along the boundaries of the aggregate. Rims show normal zoning and skeletal crystal form suggestive of rapid growth (arrow). (**D**) Plagioclase on the edge of a mafic crystal aggregate (sample SCL-55E; DHP unit). The crystal has a calcic core (An_{74-84}). There is a sharp interface between core and rim marked by a sodic shift of ~20 mol% An (at a), skeletal region (from a to b), and a normally zoned outer rim (from b to c). The skeletal region was probably formed by rapid growth. Also note textural heterogeneity in the groundmass surrounding the crystal.

these hypotheses in a given occurrence. Rapid growth textures should not disturb underlying zones (Figs. 7A, 8D) and may lead to skeletal crystal terminations (Figs. 5C, 5D). Conversely, resorption should truncate underlying zones (Figs. 3A, 5B, 5C) and progress inward from crystal margins along cracks and grain boundaries (Figs. 3D, 8A). Evaluation of compositional information is also critical in distinguishing between resorption and rapid growth. If a fritted texture represents the reaction of sodic plagioclase to more calcic compositions by preferential dissolution of the sodic component (Tsuchiyama and Takahashi, 1983), analyses of the fritted region should be more calcic than those of the underlying zones (Figs. 3A, 3D, 5B, 5C, 8A). Conversely, plagioclase formed rapidly by undercooling should be more sodic than underlying zones (Figs. 7A, 7B, 8D) (Smith and Lofgren, 1983).

Textural and compositional relations in Clear Lake dacites indicate that fritted textures have formed by both reaction and rapid growth (compare Figs. 5B, 8D), but a fritted texture formed by the reaction of sodic plagioclase to a more calcic composition appears to be much more common. The occurrence of partially fritted grains with sodic cores in quenched andesitic inclusions demonstrates that this texture forms when sodic plagioclase (derived from the silicic end-member) is assimilated by mafic liquids (see Figs. 3F, 8A). In these grains, fritted regions truncate early-formed zones, and crystals have clear overgrowths with compositions that match those of plagioclase microphenocrysts in quenched inclusions (Figs. 5C, 5D). Similar partially or completely fritted grains in dacites have remnants of quenched inclusion groundmass preserved in embayments (Fig. 8B), suggesting that such crystals have been cycled through quenched inclusions, which have since been disaggregated.

Sanidine zoning. The abrupt increase in Ba, Ca, and Al in sanidine in areas outside of the rounded or ragged interfaces (Fig. 7A) appears to result from dissolution of sanidine, followed by the growth of more Ba-rich compositions. Ba (and Ca) zoning in sanidine may be more resistent to solid-state reequilibration than K-Na zoning because Ba^{2+} and Ca^{2+} are coupled to Al^{3+} in a manner similar to Ca^{2+} in plagioclase (Grove et al., 1984). The slow rate of coupled Ba-Al and Ca-Al diffusion in sanidine is consistent with the observation that Ba zoning is more commonly preserved in potassium feldspar in plutonic rocks than is Na-K zoning (Vernon, 1986). We propose the following explanation for Ba zoning. The first growth of sanidine following an episode of dissolution is likely to be Ba rich because the concentration of Ba would be higher in the dissolution boundary layer than in the bulk melt (provided it was not stripped by convection or removed by diffusion). Subsequent growth would deplete Ba in the boundary layer, eventually lowering its concentration. Thus we consider the pattern of Ba zoning in sanidine to be analogous to certain types of Ca zoning in plagioclase.

Sanidine reaction textures. The plagioclase mantles on sanidine in dacite lavas at Clear Lake bear a striking resemblance to a rapakivi texture in granitic rocks (Stimac and Wark, 1992). Hibbard (1981) examined numerous examples of rapakivi texture in plutonic rocks and concluded that mixing of mafic and felsic magmas offered the best mechanism for producing it. He noted that many plutonic rocks that contain mantled potassium feldspar also contain mafic inclusions. More recent studies have concluded that the rapakivi texture in fine-grained mafic to intermediate composition inclusions results from magma mixing (Vernon, 1986, 1990; Bussy, 1990).

Hibbard (1981) proposed a scenario for the formation of rapakivi texture where mafic magma was injected into felsic magma and partially quenched by it, producing mafic inclusions and hybrid magma. Potassium feldspar derived from the felsic magma was resorbed and eventually overgrown by dendritic plagioclase as it came into contact with hybrid magma. Hibbard interpreted plagioclase mantles on potassium feldspar and a fritted texture in plagioclase phenocrysts as resulting from rapid growth by undercooling (Lofgren, 1974a). At Clear Lake, mantle compositions are too sodic to have formed in hybrid andesite (Fig. 2). In fact, sanidine in andesitic inclusions typically exhibits evidence of dissolution, and plagioclase mantles have a fritted texture at their margins, implying sodic mantles were also undergoing reaction. Using the distribution of mantles, their textures, and compositions as a basis, we suggest that the growth of mantles may be related to the formation of dissolution boundary layers on sanidine. Bussy (1990) independently suggested a similar mechanism for rapakivi formation using observations from plutonic rocks.

Augite coronas on quartz. At Clear Lake, it seems likely that augite coronas formed in hybrid andesitic magma derived by the mixing of quartz-bearing silicic magma with basaltic andesite. Similar coronas have been described from basaltic to dacitic rocks worldwide and reproduced experimentally in mafic liquids by a number of workers (Sato, 1975; Watson, 1982; Ussler and Glazner, 1987; Glazner et al., 1988). Sato (1975) proposed a model for corona growth by diffusion in a boundary layer surrounding quartz. He documented uphill diffusion of alkalis into glass surrounding augite and concluded that the high alkali content of the boundary layer increased the chemical potential of CaO relative to the groundmass, resulting in the growth of augite, even in magmas not saturated with clinopyroxene. Quenched inclusions in some dacitic units at Clear Lake representing hybrid andesitic magma clearly record this process (Stimac, 1991). They contain quartz with augite coronas, as well as sodic plagioclase with the fritted texture described above. It is also possible that some augite coronas grew in more silicic hybrid magmas that were undersaturated with respect to quartz. The presence of abundant fragments of augite coronas in dacites indicates that quartz dissolution sometimes went to completion or that overgrowth textures were disrupted after formation.

Mafic end-member

Plagioclase zoning. The zoning pattern and compositional range of calcic cores of phenocrysts in Clear Lake dacite lavas is consistent with crystallization from basaltic andesite (Fig. 2). The marked shift to a more evolved composition, followed by strong normal zoning, is compatible with rapid undercooled crystallization of plagioclase from a restricted supply of liquid. Lofgren (1974b) experimentally produced similar patterns of discontinuous normal zoning, followed by continuous reverse zoning in plagioclase by rapid drops in temperature (discussed by Smith and Lofgren, 1983, p. 157, Fig. 5). Lofgren's experiments indicate that the magnitude of the normal shift was directly proportional to the magnitude of the temperature drop. In their experiments, each temperature drop was followed by a period of isothermal crystallization that resulted in even to reverse zoning. Lofgren (1974b) argued that rapid temperature drops result in the growth of plagioclase more sodic than that predicted at equilibrium, and that continuous reverse zoning forms as the system reapproaches equilibrium. A stepwise cooling history is exactly what is expected for a calcic plagioclase phenocryst growing from a mafic magma that was suddenly blended with, and partially quenched by, more felsic magma, and it may explain small compositional reversals present in some crystals just outside the core-rim interface (see Figs. 6, 7, 8 in Stimac et al., 1990; Figs. 7B, 7D in this work). Such sodic shifts are observed in large crystals in both quenched inclusions and mafic crystal aggregates in dacite lavas, suggesting that mafic crystal aggregates were once part of quenched inclusions or that they underwent a similar stage of undercooled crystallization (compare Figs. 7B, 7D, 8). The widespread occurrence of similar sodic shifts and strong normal zoning at crystal rims in calc-alkaline rocks (Smith and Lofgren, 1983; Barbarin, 1990; Blundy and Shimizu, 1991) suggests that recycling of mafic-derived plagioclase

into more silicic magmas is both common and widespread.

Disequilibrium textural features of dacite lavas

The large degree of thermal and chemical disequilibrium induced by the interaction of subequal volumes of mafic and felsic magma is recorded by textures and the mineral assemblages in dacite lavas at Clear Lake (Figs. 3–8). Not only do end-member phenocrysts preserve distinct compositions and styles of textural reequilibration, but comparison of textures in quenched inclusions with those in the dacite host provide constraints on the nature of the mixing process. The phenocryst assemblage derived from the felsic end-member responded to mixing mainly by dissolution or reaction. Disequilibrium resulted in (1) simple dissolution, (2) partial reaction progressing inward from crystal margins, (3) local internal melting of crystals, and (4) formation of mantles or coronas by diffusion-limited reactions in dissolution boundary layers at the margins of crystals. Silicic end-member crystals in andesitic inclusions consistently display extreme disequilibrium, whereas those in dacite exhibit the complete range of textures described.

The mafic end-member magma responded to mixing mainly by undercooled crystallization, resulting in quenched inclusions and disseminated crystalline debris with compositions intermediate between the end-member phenocryst compositions (Figs. 3E, 3F). Inclusion microphenocrysts are characterized by dendritic or skeletal growth forms. Plagioclase microphenocrysts in quenched inclusions show strong normal zoning and are characterized by dendritic or skeletal growth forms. Clino- and orthopyroxene microphenocrysts in quenched inclusions commonly occur as intergrowths, inferred to have formed by epitaxial nucleation in an undercooled environment (Kuno, 1950). Calcic plagioclase phenocrysts in quenched inclusions and mafic aggregates show abrupt shifts to more evolved compositions. Compositions of rims on the calcic plagioclase phenocrysts match those of plagioclase microphenocrysts in the groundmass of inclusions. Mg-rich olivine is rimmed by orthopyroxene or amphibole of the same composition as that in the groundmass of inclusions (Fig. 3A). Identical zoning styles and overgrowth textures are present in both mafic end-member minerals in quenched inclusions and the dacite host. These textures and zoning patterns reflect rapid growth from liquid in an undercooled environment.

Crystal textures and their environment of formation

The variety of mineral textures and compositions in Clear Lake dacite lavas and their common distribution in lavas along with hybrid andesite inclusions implies to us distinctly different environments of formation for some textures. This observation of different textures occurring within the same hand specimen (or even thin section) can be reconciled by a multistage mixing model for dacite formation such as the one illustrated in Figure 9. In this simplified model, mixing is triggered by the influx of basaltic andesite into a crystal-rich silicic magma body.

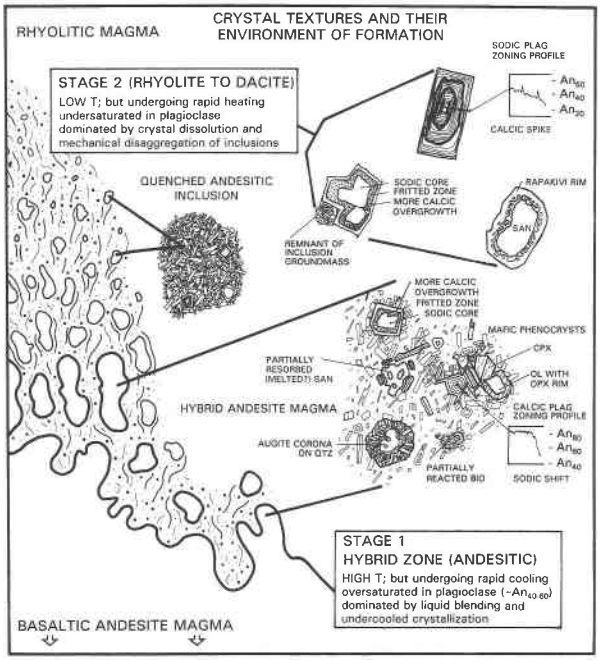

Fig. 9. Relationships between disequilibrium textures and their environments of formation. Stages 1 and 2 may occur on the scale of magma body, or locally at a contact between mafic and felsic magma. Individual crystals may experience one or more mixing events, including either or both stages. Disequilibrium textures ascribed to stage 1 processes include a fritted texture in sodic plagioclase, augite coronas on quartz, and dissolution of sanidine. Disequilibrium textures ascribed to stage 2 include simple dissolution and compositional reversals in plagioclase, sanidine, and pyroxene, and plagioclase mantles on sanidine. Rapid growth and reaction textures in the mafic end-member are attributed primarily to stage 1.

Blending of basaltic andesite and rhyolite dominates the early stages of mafic-felsic magma interaction (stage 1). As the mafic magma assimilates silicic liquid and crystals, it undergoes rapid crystallization, eventually segmenting into discrete hybrid inclusions in a more silicic host (compare with Kouchi and Sunagawa, 1985; Nixon, 1988a). As crystallization proceeds and the viscosity of inclusions and host become similar, inclusions suffer extensive disaggregation, contributing crystalline debris and hybrid liquid to mixed dacite (stage 2) (compare with Thompson and Dungan, 1985; Clynne, 1989; Poli and Tommasini, 1991).

Zoning and reaction textures of plagioclase provide clear evidence for the nature of these two environments (Fig. 9). Fritting occurs when sodic plagioclase was assimilated by hybrid magmas formed during the initial stages of mafic-felsic magma interaction (stage 1). These intermediate magmas rapidly lose heat as they hybridize with adjacent silicic magma and crystallize abundant plagioclase and pyroxene, eventually forming partially quenched inclusions. Tsuchiyama (1985) showed experimentally that sodic plagioclase immersed in a magma saturated with more calcic plagioclase develops fritted texture. In

most natural examples, fritted regions are overgrown by intermediate composition plagioclase as their host magma crystallizes (Fig. 9). In contrast, sodic crystals not directly incorporated into andesitic hybrids experience a rapid increase in temperature, possibly followed by a relatively small change in liquid composition as their silicic host magma undergoes mechanical mixing with inclusion debris (stage 2). Sodic crystals with calcic spikes (simple dissolution followed by compositional reversal) record this process. Factors leading to renewed growth of a more calcic composition probably include (1) changes in liquid composition resulting from limited liquid blending, (2) the effects of fractionation and cooling following mixing (Nixon, 1988a), and (3) growth from the dissolution boundary layer previously enriched in plagioclase constituents (Kolisnik, 1990).

Although some homogenization undoubtedly occurs in conduits, careful study of calc-alkaline plutonic rocks has revealed the same range of textural features as present in extrusive equivalents (Frost and Mahood, 1987; Vernon, 1990; Blundy and Shimizu, 1991; Zorpi et al., 1991). Our observations at Clear Lake suggest that, provided mafic input is sufficient, mechanical mixing of mafic and silicic magma is remarkably efficient, despite initially large contrasts in composition and viscosity.

Acknowledgments

This work is a contribution from the Laser Laboratory at Queen's University, supported by National Sciences and Engineering Research Council of Canada (NSERC) grant no. 0656. Additional financial support for this study was provided by NSERC grant no. 8709 (T.H.P.). The cost of field work was defrayed in part by a grant from Sigma Xi (J.A.S.). We thank J.M. Donnelly-Nolan, B.C. Hearn, Jr., and D. Jacobs for assistance in our study of the Clear Lake Volcanics. Useful reviews were provided by M. Clynne, S. Linneman, and C. Bacon. Thanks also to A. Kolisnik and D. Wark for stimulating discussions concerning mineral zoning and reaction patterns. D. Crawford provided valuable assistance with manuscript preparation.

References cited

Albee, A.L., and Ray, L. (1970) Correction factors for electron microanalysis of silicates, oxides, carbonates, phosphates and sulphates. Analytical Chemistry, 42, 1408–1414.

Anderson, A.T., Jr. (1976) Magma mixing: Petrologic process and volcanological tool. Journal of Volcanology and Geothermal Research, 1, 3–33.

——— (1983) Oscillatory zoning of plagioclase: Nomarski interference contrast microscopy of etched sections. American Mineralogist, 68, 125–129.

——— (1984) Probable relations between plagioclase zoning and magma dynamics, Fuego Volcano, Guatemala. American Mineralogist, 69, 660–676.

Anderson, C.A. (1936) Volcanic history of the Clear Lake area, California. Geological Society of America Bulletin, 47, 629–664.

Bacon, C.R. (1986) Magmatic inclusions in silicic and intermediate volcanic rocks. Journal of Geophysical Research, 91, 6091–6112.

Bacon, C.R., and Metz, J. (1984) Magmatic inclusions in rhyolites, contaminated basalts, and compositional zonation beneath the Coso volcanic field, California. Contributions to Mineralogy and Petrology, 85, 346–365.

Barbarin, B. (1990) Plagioclase xenocrysts and mafic magmatic enclaves in some granitoids of the Sierra Nevada Batholith, California. Journal of Geophysical Research, 95, 17747–17756.

Bence, A.E., and Albee, A.L. (1968) Empirical correction factors for electron microanalysis of silicates and oxides. Journal of Geology, 76, 382–386.

Blundy, J.D., and Shimizu, N. (1991) Trace element evidence for plagioclase recycling in calc-alkaline magmas. Earth and Planetary Science Letters, 102, 178–197.

Brice, J.C. (1953) Geology of the Lower Lake Quadrangle, California. California Division of Mines Bulletin, 166, 34–49.

Bussy, F. (1990) The rapakivi texture of feldspars in a plutonic mixing environment: A dissolution-recrystallization process? Geological Journal, 25, 319–324.

Clynne, M.A. (1989) Disaggregation of quenched magmatic inclusions contributes to chemical diversity in silicic lavas of Lassen Peak, California. New Mexico Bureau of Mines and Mineral Resources Bulletin, 131, 54.

Donnelly-Nolan, J.M., Hearn, B.C. Jr., Curtis, G.H., and Drake, R.E. (1981) Geochronology and evolution of the Clear Lake volcanics. U.S. Geological Survey Professional Paper 1141, 47–66.

Eichelberger, J.C. (1978) Andesitic volcanism and crustal evolution. Nature, 275, 21–27.

Frost, T.P., and Mahood, G.A. (1987) Style of mafic-felsic magma interaction: The Lamarck Granodiorite, Sierra Nevada, California. Geological Society of America Bulletin, 99, 272–291.

Glazner, A.F., Ussler, W., III, and Mies, J.W. (1988) Fate of granitic minerals in mafic magmas. Eos, 69, 1504.

Glazner, A.F., Ussler, W., III, and Mathis, A.C. (1990) Interpretation of plagioclase texture in volcanic rocks. Eos, 71, 1678.

Grove, T.L., and Donnelly-Nolan, J.M. (1986) The evolution of young silicic lavas at Medicine Lake Volcano, California: Implications for the origin of compositional gaps in calc-alkaline series lavas. Contributions to Mineralogy and Petrology, 92, 281–302.

Grove, T.L., Baker, M.B., and Kinzler, R.J. (1984) Coupled CaAlNaSi diffusion in plagioclase feldspar: Experiments and application to cooling rate speedometry. Geochimica et Cosmochimica Acta, 48, 2113–2121.

Hearn, B.C., Jr., Donnelly-Nolan, J.M., and Goff, F.E. (1976) Preliminary geologic map and cross-section of the Clear Lake volcanic field, Lake County, California. U.S. Geological Survey Open-File Report 76-751.

——— (1981) The Clear Lake Volcanics: Tectonic setting and magma sources. U.S. Geological Survey Professional Paper 1141, 25–45.

Heiken, G., and Eichelberger, J.C. (1980) Eruptions at Chaos Crags, Lassen Volcanic National Park, California. Journal of Volcanology and Geothermal Research, 7, 443–481.

Hibbard, M.J. (1981) The magma mixing origin of mantled feldspars. Contributions to Mineralogy and Petrology, 76, 158–170.

Homma, F. (1932) Über das Ergebnis von Messungen an zonaren Plagioklasen aus Andesiten mit Hilfe des Universaldrehtisches. Schweizerische mineralogische und petrographische Mitteilungen, 12, 345–352.

——— (1936) Classification of zonal structure in plagioclase. Memorial College of Science, Kyoto Imperial University Serial B11, 135–155.

Huppert, H.E., Sparks, R.S.J., and Turner, J.S. (1982) Effects of volatiles on mixing in calc-alkaline magma systems. Nature, 297, 554–557.

——— (1984) Some effects of viscosity on the dynamics of replenished magma chambers. Journal of Geophysical Research, 89, 6857–6877.

Kolisnik, A. (1990) Phenocryst zoning and heterogeneity in andesites and dacites of Volcán Popocatépetl, Mexico, 247 p. M.Sc. thesis, Queen's University, Kingston, Ontario, Canada.

Kouchi, A., and Sunagawa, I. (1985) A model for mixing basaltic and dacitic magmas as deduced from experimental data. Contributions to Mineralogy and Petrology, 89, 17–23.

Koyaguchi, T. (1985) Magma mixing in a conduit. Journal of Volcanology and Geothermal Research, 25, 365–369.

Kuno, H. (1950) Petrology of Hakone volcano and adjacent areas, Japan. Geological Society of American Bulletin, 61, 957–1020.

Kuo, L., and Kirkpatrick, R.J. (1982) Pre-eruption history of phyric basalts from DSDP Legs 45 and 46: Evidence from morphology and zoning patterns in plagioclase. Contributions to Mineralogy and Petrology, 79, 13–27.

Lofgren, G.E. (1974a) An experimental study of plagioclase crystal morphology: Isothermal crystallization. American Journal of Science, 274, 243–273.

——— (1974b) Temperature induced zoning in synthetic plagioclase feld-

spar. In W.W. Mackenzie and J. Zussman, Eds., The feldspars, p. 362–375. Manchester University Press, Manchester, England.

Lofgren, G.E., and Norris, N. (1981) Experimental duplication of plagioclase sieve and overgrowth textures. Geological Society of America Abstracts with Programs, 13, 498.

Loomis, T.P. (1982) Numerical simulations of crystallization processes of plagioclase in complex melts: The origin of major and oscillatory zoning in plagioclase. Contributions to Mineralogy and Petrology, 81, 219–229.

Nixon, G.T. (1988a) Petrology of the younger andesites and dacites of Iztaccíhuatl volcano, Mexico: I. Disequilibrium phenocryst assemblages as indicators of magma chamber processes. Journal of Petrology, 29, 213–264.

——— (1988b) Petrology of the younger andesites and dacites of Iztaccíhuatl volcano, Mexico: II. Chemical stratigraphy, magma mixing, and the composition of basaltic magma influx. Journal of Petrology, 29, 265–303.

Nixon, G.T., and Pearce, T.H. (1987) Laser-interferometry study of oscillatory zoning in plagioclase: The record of magma mixing and phenocryst recycling in calc-alkaline magma chambers, Iztaccíhuatl volcano, Mexico. American Mineralogist, 72, 1144–1162.

Oldenburg, C.M., Spera, F.J., Yuen, D.A., and Sewell, G. (1989) Dynamic mixing in magma bodies: Theory, simulations, and implications. Journal of Geophysical Research, 94, 9215–9236.

Pearce, T.H. (1984a) Multiple frequency laser interference microscopy: A new technique. The Microscope, 32, 69–81.

——— (1984b) Optical dispersion and zoning in magmatic plagioclase: Laser-interference observations. Canadian Mineralogist, 22, 383–390.

Pearce, T.H., and Clark, A.H. (1989) Nomarski interference contrast observations of textural details in volcanic rocks. Geology, 17, 757–759.

Pearce, T.H., and Kolisnik, A.M. (1990) Observations of plagioclase zoning using interference imaging. Earth Science Reviews, 29, 9–26.

Pearce, T.H., Russell, J.K., and Wolfson, I. (1987) Laser-interference and Nomarski interference imaging of zoning profiles in plagioclase from the May 18, 1980, eruption of Mount St. Helens. American Mineralogist, 72, 1131–1143.

Phemister, J. (1934) Zoning in plagioclase feldspar. Mineralogical Magazine, 23, 541–555.

Poli, G.E., and Tommasini, S. (1991) Model for the origin and significance of microgranular enclaves in calc-alkaline granitoids. Journal of Petrology, 32, 657–666.

Sakuyama, M. (1981) Petrological study of the Myoko and Kurochime volcanoes, Japan: Crystallization sequences and evidence for magma mixing. Journal of Petrology, 22, 553–583.

Sato, H. (1975) Diffusion coronas around quartz xenocrysts in andesites and basalts from Tertiary volcanic region in northeastern Shikoku, Japan. Contributions to Mineralogy and Petrology, 50, 40–64.

Sibley, D.F., Vogel, T.A., Walker, B.M., and Byerly, G. (1976) The origin of oscillatory zoning in plagioclase: A diffusion and growth controlled model. American Journal of Science, 276, 275–284.

Smith, J.V., and Brown, W.L. (1988) Feldspar minerals, vol. 1 (2nd edition), 828 p. Springer-Verlag, Berlin.

Smith, R.K., and Lofgren, G.E. (1983) An analytical and experimental study of zoning in plagioclase. Lithos, 1, 153–168.

Sparks, R.S.J., and Marshall, L.A. (1986) Thermal and mechanical constraints on mixing between mafic and silicic magmas. Journal of Volcanology and Geothermal Research, 29, 99–124.

St. Seymour, K., Vlassopoulos, D., Pearce, T.H., and Rice, C. (1990) The record of magma chamber processes in plagioclase phenocrysts at Thera Volcano, Aegean Volcanic Arc, Greece. Contributions to Mineralogy and Petrology, 104, 73–84.

Stimac, J.A. (1991) Evolution of the silicic magmatic system at Clear Lake, California, from 0.6 to 0.3 Ma, 399 p. Ph.D. dissertation, Queen's University, Kingston, Ontario, Canada.

Stimac, J.A., and Pearce, T.H. (1989) Origin of dacite lavas at Clear Lake, California: Disseminated of mafic crystalline debris in silicic magma. Eos, 70, 1409.

Stimac, J.A., and Wark, D.A. (1992) Plagioclase mantles on sanidine in silicic lavas, Clear Lake, California: Implications for the origin of rapakivi texture. Geological Society of America Bulletin, 104, 728–744.

Stimac, J.A., Pearce, T.H., Donnelly-Nolan, J.M., and Hearn, B.C. Jr. (1990) Origin and implications of undercooled andesitic inclusions in rhyolites, Clear Lake Volcanics, California. Journal of Geophysical Research, 95, 17729–17746.

Thompson, R., and Dungan, M.A. (1985) The petrology and geochemistry of the Handkerchief Mesa mixed magma complex, San Juan Mountains, Colorado. Journal of Volcanology and Geothermal Research, 26, 251–274.

Tsuchiyama, A. (1985) Dissolution kinetics of plagioclase in melt of the system diopside-albite-anorthite and the origin of dusty plagioclase in andesites. Contributions to Mineralogy and Petrology, 89, 1–16.

Tsuchiyama, A., and Takahashi, E. (1983) Melting kinetics of a plagioclase feldspar. Contributions to Mineralogy and Petrology, 84, 345–354.

Turner, J.S., and Campbell, I.H. (1986) Convection and mixing in magma chambers. Earth Science Reviews, 23, 255–352.

Ussler, W., III, and Glazner, A.F. (1987) Origin of augite coronas around quartz xenocrysts in basalts and andesites. Eos, 19, 874.

——— (1989) Phase equilibria along a basalt-rhyolite mixing line: Implications for the origin of calc-alkaline intermediate lavas. Contributions to Mineralogy and Petrology, 101, 232–244.

Vernon, R.H. (1986) K-feldspar megacrysts in granites—phenocrysts, not porphyroblasts. Earth Science Reviews, 23, 1–63.

——— (1990) Crystallization and hybridism in microgranitoid enclave magmas: Microstructural evidence. Journal of Geophysical Research, 95, 17849–17859.

Watson, E.B. (1982) Basalt contamination by continental crust: Some experiments and models. Contributions to Mineralogy and Petrology, 80, 73–87.

Wilcox, R.E. (1944) Rhyolite-basalt complex on Gardiner River, Yellowstone Park, Wyoming. Geological Society of America Bulletin, 55, 1047–1080.

Zorpi, M.J., Coulon, C., and Orsini, J.B. (1991) Hybridization between felsic and mafic magmas in calc-alkaline granitoids—a case study in northern Sardinia, Italy. Chemical Geology, 92, 45–86.

Manuscript received May 20, 1991
Manuscript accepted March 13, 1992